https://doi.org/10.1016/j.jobe.2023.106874

A novel indirect evaporative cooler with porous media under dual spraying modes: a comparative analysis from energy, exergy, and environmental perspectives

Wenchao Shi [a,*], Hongxing Yang [a], Xiaochen Ma [a], Xiaohua Liu [b,**]

[a] Renewable Energy Research Group (RERG), Department of Building Environment and Energy Engineering, The Hong Kong Polytechnic University, Hong Kong, China

[b] Department of Building Science, Tsinghua University, Beijing, China

Abstract

Indirect evaporative cooling (IEC), which cools the air through the physical process, is regarded as one of the high-efficient air conditioning (AC) devices. The reliable performance of traditional IEC is maintained by consistent water spraying, consuming much energy and hindering further performance improvement. In this regard, we proposed a novel indirect evaporative cooler with porous media on the secondary air channel (PIEC) to mitigate the dependence on the water spraying. For the PIEC, periodic spraying can be realized owing to the water storage capacity of porous media. However, the performance comparison between periodic spraying and traditional consistent spraying is rarely carried out although the two modes have been achieved, which promotes this research. In this study, the PIEC model with consistent spraying and periodic spraying was briefly described based on our previous results. According to the results from the established model, the PIEC performance was analyzed and compared under dual spraying modes from the energy, exergy, and environmental (3E) perspectives. It is demonstrated that periodic spraying can significantly improve the system COP by 58.7% at the cost of tiny temperature fluctuations. Meanwhile, the periodic mode can increase the exergy efficiency and lessen the exergy loss ratio in the studied cases. Eventually, the PIEC system using periodic spraying can annually reduce 24.2 kg of CO_2 emissions compared with the traditional consistent mode, indicating the better environmental benefit.

* Corresponding author.
** Corresponding author.
E-mail addresses:
wenchao511.shi@connect.edu.hk (W. Shi)
lxh@tsinghua.edu.cn (X. Liu)

Graphical Abstract

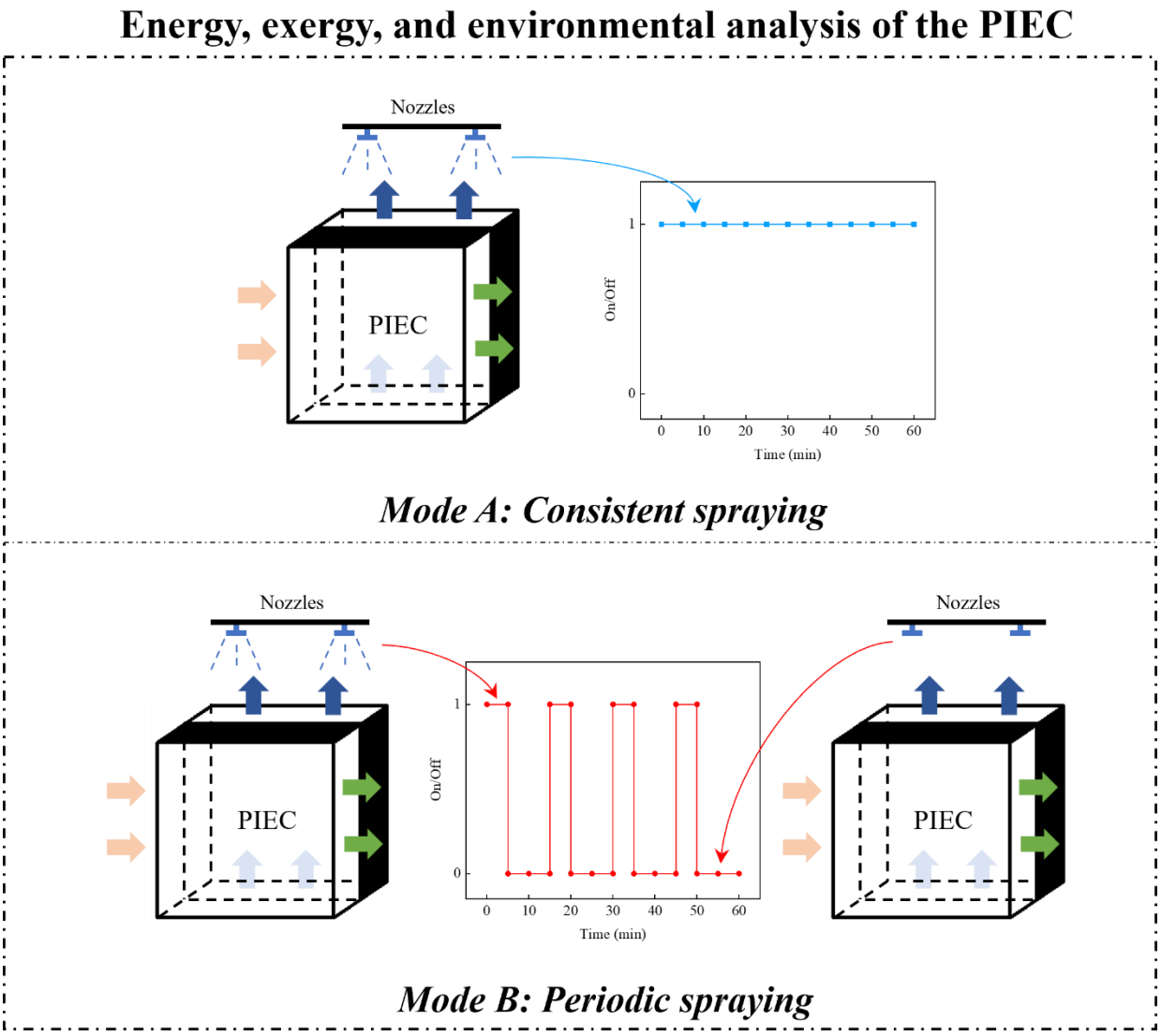

Keywords

Air conditioning; Porous material; Dual-mode spraying plan; Indirect evaporative cooling; 3E evaluation

Nomenclature

c_{pa}	Specific heat capacity of air, J/(kg·K)
d	Channel gap distance, mm
D_{va}	Diffusivity between vapor and air, m2/s
E	Energy, W
Ex	Exergy, W/Wh
f	Emission coefficient, kg/kWh
H	Height, mm
h_{fg}	Latent heat of evaporation, J/kg
i	Enthalpy, kJ/kg
k	Thermal conductivity, W/(m · K)
L	Length, mm
m	Mass flowrate, kg/s
n	Mass flux, kg/(m^2 · s)
Nu	Nusselt number
P	Pressure, Pa
S	Saturation of phase
T	Temperature, K
t	Temperature, ℃
u	Velocity, m/s
W	Power, W
Q	Cooling capacity, W

Greek symbols

ε	Porosity
η	Efficiency
μ	Dynamic viscosity, Pa · s
τ	Time, s
ρ	Density, kg/m^3

Abbreviations

1, 2, 3-D	One, two, three dimensional
AC	Air conditioning
AHU	Air handling unit
Con.	Consistent/Continuous/Consecutive/Stable spraying
COP	Coefficient of performance
DEC	Direct evaporative cooling
DIEC	Dew-point indirect evaporative cooler
DX	Direct expansion
IEC	Indirect evaporative cooler
Per.	Periodic/Intermittent/Recurrent/Recurring spraying
PIEC	Porous indirect evaporative cooler
RH	Relative humidity, %
SEM	scanning electron microscope

Subscripts

a	air
ef	Effective
loss	Destruction
in	Inlet
out	Outlet
p	Primary air
s	Secondary air
sen	Sensible
lat	Latent
ther	Thermal
chem	Chemical
g	Gas phase
l	Liquid phase
s	Solid phase

1. Introduction

Achieving the carbon peaking and carbon neutrality goals requires not only the development and full use of renewable energy but the reduction of energy consumption by the current equipment [1, 2]. Air conditioning (AC) systems serve to create a comfortable indoor environment but at the cost of consuming much energy in buildings. Sustainable and environmental-friendly air cooling approaches, therefore, attract more attention. Indirect evaporative cooler (IEC), free of vapor compression and any chemical refrigerant, has received a wide preference for energy saving in the past decades, especially in hot and arid areas [3-6]. As depicted in Fig. 1, primary and secondary air branches are blown horizontally and vertically into the heat exchanger. Water is pumped from the reservoir and distributed by the nozzles to the channel surface. The air passes the secondary channel and promotes the attached liquid membrane to evaporate owing to the humidity ratio difference. Evaporation takes away the latent heat so as to reduce the temperature of the impermeable metal sheet, and then the neighboring primary air is chilled down through convective heat transfer [7, 8].

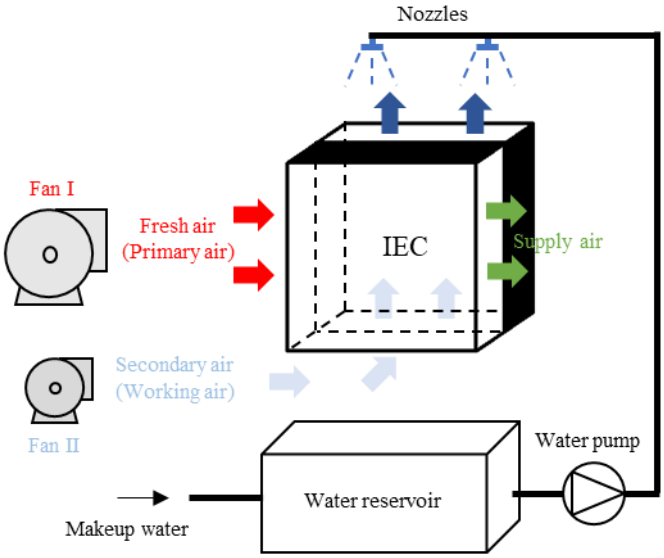

Fig. 1 The structure and components of an IEC system

To begin with, theoretical models of the various single and hybrid IEC systems were carried out with experiments to assess their thermal performance [9-11]. Then, the energy and exergy performance can be analyzed based on the initial results [12-14]. Some research further considered economic and environmental issues [15, 16]. For instance, Lin et al. developed a 2-D dew point counter-flow IEC model and discussed the exergy flow, efficiency, and efficiency ratio [17]. Li et al. established three IEC numerical models in diverse airflow arrangements, and the exhaust air was recovered as the secondary air. They reported that irreversible primary air heat transfer and secondary air mass transfer caused more than 90% of the exergy loss [18]. Ratlamwala and Dincer analyzed trends of energy and exergy efficiencies for various psychometric processes based on three different definitions, including evaporative cooling that occurs in the secondary air channel, indicating the importance of definition selection [19]. Kousar et al. conducted experiments on the counter-flow and cross-flow IECs in three

operating ranges, demonstrating that the cross-flow IEC system has better exergy efficiency and less CO_2 emissions [20]. Zhang et al. analyzed the energy, exergy, economic and environmental (4E) performance of a novel cross-flow IEC diffused with liquid desiccant in the supply air side (IECL). Results showed that IECL had better energy and exergy (2E) efficiencies than normal IEC because more water content can be removed from the air. The favorable profitability and environmental benefits of the IELC were also mentioned [21]. Rao and Datta evaluated single and multi-stage evaporative cooling systems from the perspective of exergy, sustainability, and enviro-economic based on the climate zone in India. The IEC-DEC-DX system was deemed as the most suitable mode with better exergy efficiency and environmental benefits [22]. Yang et al. developed an external-cooling IEC and compared it with two traditional IEC using 2E analysis. The energy-saving rate of the new one ranged from 19.1% to 48.5% in typical summer conditions, and the exergy destruction of it was only 50% to 70% compared with the baseline case [23]. The 4E evaluation was made on two types of regenerative evaporative coolers in four configurations. Besides, the 4E performance of the IEC with several surface modifications was also measured. The capsule-embossed format of surfaces could contribute to the best COP and exergy efficiency [24, 25].

Porous media has started to be employed for performance enhancement in several types of IECs [26, 27]. With regard to the research on IEC with porous material, Chen et al. compared several porous plant fiber-polymer composites used for IEC heat transfer sheets. The wicking height, diffusivity, absorption, and moisture release were examined. A counter-flow prototype was tested under recurrent spraying plans, revealing the practicability of porous material application in IEC [28]. Shi et al. proposed a cross-flow PIEC sintered porous layer on the working channel surface. Lab tests were conducted to measure the performance of a prototype [29, 30]. Results showed that cyclic spraying was achieved with up to 161.2% COP improvement [31]. Besides, the tubular IEC and the heat-pipe-based IEC using porous ceramic were developed and fabricated [32, 33].

Table 1 Summary of the previous IEC research on "E" and this study

Research	"E" analysis	Spraying mode	Features
Pakari and Ghani [34]	1	Con.	Impacts of extraction ratio, inlet air properties, and geometric size on wet-bulb efficiency are analyzed based on 1-D and 3-D counter-flow IEC models.
Lin et al. [17]	1, 2	Con.	Effects of supply air status and operating conditions on "2E" of the counter-flow IEC were analyzed.
Li et al. [18]	1, 2	Con.	Influences of variable working conditions on "2E" were assessed for IECs in three traditional configurations with heat recovery.
Kashyap et al. [35]	1, 2, 3, 4	Con.	"4E" of counter and cross-flow of IECs with eight configurations were compared based on varied extraction ratios, airflow rates, and

			channel gaps.
Kousar et al. [20]	1, 2, 3, 4	Con.	Comparisons of "4E" were carried out on cross-flow IECs by changing input air properties and operation levels.
Zhang et al. [21]	1, 2, 3, 4	Con.	The IEC with sprayed liquid desiccant on primary air channels and the normal IEC were examined from "4E".
This study	1, 2, 4	Con.; Per.	"3E" analysis of the cross-flow PIEC was conducted under ranged inlet air conditions considering traditional and periodic spraying modes.

Note: 1 - energy; 2 - exergy; 3 - economic; 4 - environmental.

Con.: Consistent/Continuous/Consecutive/Stable spraying mode.

Per.: Periodic/Intermittent/Recurrent/Recurring spraying mode.

Comparisons among some published studies and this study on the "E" analysis of indirect evaporative coolers have been summarized in Table 1. It can be identified that the normal IECs in diverse airflow arrangements and configurations have been investigated in full swing. However, to our best knowledge, two research gaps can be identified. In the first place, the detailed 3E evaluation of the PIEC is lacking, even though it has been proposed and preliminarily investigated. In addition, the intermittent spraying is unique in PIEC, but there is no comparison for PIEC from the 3E perspectives considering the traditional spraying mode and this new spraying mode, which is also the motivation of this work.

To address the above research gaps, this study was carried out in the following sequences. Firstly, the model of the novel plate-type cross-flow PIEC was briefly described with the proposal of dual spraying modes based on our previous research. Secondly, the energy and exergy of this heat exchanger with various inlet conditions were evaluated under consistent and periodic spraying conditions, respectively. Then, according to the latest emissions factor, the environmental contributions of the PIEC in two modes were compared with the conventional air conditioning system. Finally, limitations, future works, and some operating recommendations were summarized.

2. Brief description of simulation models and dual-spraying modes

2.1 Description of the IEC and PIEC

The section views of two types of IECs are displayed in Fig. 2. The working principle of a traditional IEC has been illustrated in the Introduction section. The water film covers the secondary channel plate with the support of continuous spraying. Regarding the proposed PIEC (Fig. 2(b)), the porous layer is made on the secondary air channel surface, while the smooth side faces toward the primary air channel. During the spraying period, liquid water can be reserved in the porous zone. When the spraying system pauses, the PIEC can still produce cooling for some time by using the stored water.

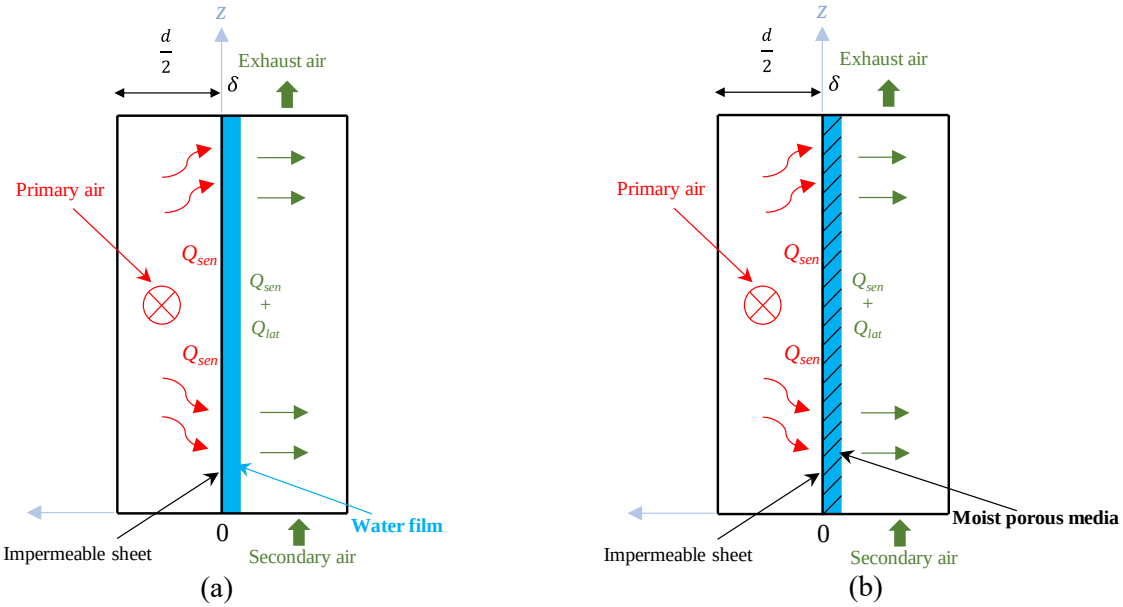

Fig. 2 Section view of (a) Normal IEC (b) PIEC

2.2 Model establishment of the PIEC

The PIEC simulation model was developed in our previous works [31]. Assumptions for model establishment are illustrated as follows: 1) No heat and mass exchanges with surroundings. 2) Working fluids are incompressible, and the velocity fields are time-independent. 3) The flow status in both the free and porous zone is deemed to be the laminar flow. 4) Porous skeleton is rigid, consecutive, and homogeneous during water-absorbing or evaporation. 5) Pores are well-distributed in similar sizes with no insulated air hole. 6) None of the chemical process exists amid solid, liquid, and gas phases. 7) Liquid water is uniformly absorbed in the porous layer. 8) The convective heat transfer in the porous layer is not considered. 9) Water content only departs from the moist porous area in the form of vapor.

Essential equations are accordingly presented to facilitate reading as well. For the spraying condition, water is sufficient for the PIEC for cooling production. The process is time-independent and in steady state. The continuity, momentum, energy, and species equations are written from Eq. (1) to Eq. (4).

$$\nabla \cdot \boldsymbol{u_i} = 0 \tag{1}$$

$$\rho_i \boldsymbol{u_i} \cdot (\boldsymbol{u_i}) = -P_i + \mu_i \nabla^2 \boldsymbol{u_i} \tag{2}$$

$$\rho_i c_{pa} \boldsymbol{u_i} \nabla \boldsymbol{t_i} = k_a \nabla^2 \boldsymbol{t_i} \tag{3}$$

where i = p, s

$$\boldsymbol{u_s} \cdot \nabla \omega_s = D_{va} \nabla^2 \omega_s \tag{4}$$

For the intermittent spraying condition, when spraying water is paused, the outlet parameters of air channels are related to the working time. Thus, time items need to be supplemented, and Eqs. (5)-(7) are used for calculation.

$$\frac{\partial \boldsymbol{u_i}}{\partial \tau} + \rho_i \boldsymbol{u_i} \cdot (\boldsymbol{u_i}) = -P_i + \mu_i \nabla^2 \boldsymbol{u_i} \tag{5}$$

$$\rho_i c_{pa} \frac{\partial \boldsymbol{t_i}}{\partial \tau} + \rho_i c_{pa} \boldsymbol{u_i} \nabla \boldsymbol{t_i} = k_a \nabla^2 \boldsymbol{t_i} \tag{6}$$

where i = p, s

$$\frac{\partial \omega_s}{\partial \tau} + \boldsymbol{u_s} \cdot \nabla \omega_s = D_{va} \nabla^2 \omega_s \tag{7}$$

When the porous layer is employed on the secondary air channel, the thermal conductivity of this novel hybrid plate is changed, and the thermal properties should also be accordingly revised as Eq. (8) and Eq. (9).

$$k_{ef} = k_s(1-\varepsilon) + k_l S_l \varepsilon + k_g S_g \varepsilon \tag{8}$$

$$(\rho C_p)_{ef} = \rho_s C_{ps}(1-\varepsilon) + \rho_l C_{pl} S_l \varepsilon + \rho_g C_{pg} S_g \varepsilon \tag{9}$$

For the porous region of PIEC, the porosity is related to the volume liquid phase, gas phase, and solid phase of the porous media, which is defined by Eq. (10). The liquid saturation can be expressed as Eq. (11), and it has the relationship with gas saturation following Eq. (12).

$$\varepsilon = \frac{\Delta V_l + \Delta V_g}{\Delta V_l + \Delta V_g + \Delta V_s} \tag{10}$$

$$S_l = \frac{\Delta V_l}{\Delta V_l + \Delta V_g} \tag{11}$$

$$S_g + S_l = 1 \tag{12}$$

The water loss from the porous area will be added in the secondary air stream in the form of vapor. From the liquid phase to the gas phase, the water content transfer process is described using Eqs. (13)-(14).

$$\frac{\partial \omega_l}{\partial \tau} + \nabla \boldsymbol{n}_l = -m_{ev} \tag{13}$$

$$\frac{\partial \omega_s}{\partial \tau} + \nabla \boldsymbol{n}_v = m_{ev} \tag{14}$$

The energy equation of the wet porous region can be formulated by Eq. (15):

$$\frac{\partial \left((\rho c_p)_{ef} \boldsymbol{t} \right)}{\partial \tau} + \nabla \left((\rho c_p)_{ef} \boldsymbol{t} \right) = \nabla \, k_{ef} (\nabla \, \boldsymbol{t}) - m_{ev} h_{fg} \tag{15}$$

In order to make the content of this study concise and focus on the 3E analysis, complicated mass transfer equations between the porous material and secondary air, as well as the boundary conditions of the PIEC model, are not presented here, which has been illustrated in detail in our previous research. The PIEC model was constructed in COMSOL Multiphysics software and validated on the lab test rig with a prototype. The prototype was made by the hybrid plates that sintering the porous nickel on the stainless-steel sheet. The porous structure and smooth surface of the prototype photographed with the

scanning electron microscope (SEM) are shown in Fig. 3 [29]. From the experiments, in addition to operating under the consistent spraying mode, it can be demonstrated that the water can be stored in the porous area to support evaporation and achieve cooling when the water spraying is interrupted. In other words, it is feasible to use the porous material for improving the water retention ability and achieving the intermittent spraying. While the simulation model predicts the outlet air status in the two adjacent channels, the results are used for conducting the "E" analysis in this study. The description of the dual spraying mode is presented with a pre-test in the next section.

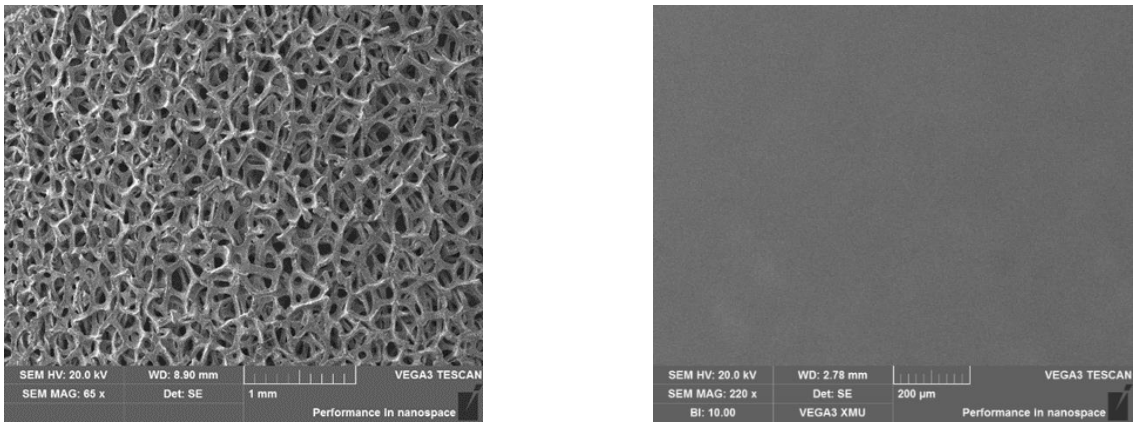

(a) (b)

Fig. 3 View of (a) porous structure and (b) smooth surface under SEM [29]

2.3 Water spraying description and pre-test results

The dual water spraying modes of the PIEC system can be categorized into consistent spraying and periodic spraying. The consistent mode requires the water system to operate all the time. Regarding the periodic spraying cycle, the spraying system only works for a short duration and pause, which is recovered when the temperature rise exceeds the threshold. Given the stable inlet air and persistent spraying conditions, the outlet temperature can be fixed when it reaches the lowest temperature because water is sufficient to support the continuous evaporation process in the secondary air channel. In this regard, the PIEC can be perceived as a normal IEC. If the periodic spraying is implemented, the cavities in the porous region afford the room to accumulate water. The evaporative cooling process can be guaranteed in the spraying period, and part of the liquid water can be absorbed in the porous zone. When the spraying system is paused, the PIEC works in the interval without sprinkling, and evaporation can be maintained for a while using the collected liquid water so as to defer the outlet temperature growth. However, the temperature is still going to slowly increase due to the limited water storage, which can only descend by recovering the water supply in the next cycle. In this study, the temperature rise of 0.5°C is determined as the threshold for judging whether the spraying is started for the next cycle, which can save the pump operating time and prevent the spraying system from switching between on/off modes frequently, thus reducing its impact on the pump useful life. The spraying duration is 120 s when the water needs to be supplied again at the threshold value.

A pre-test is carried out to illustrate the two spraying mode with the input parameters of $t_{p,in}$ =

30℃, $RH_{p,in}$ = 40%, u_p =3 m/s, $t_{s,in}$ = 25℃, $RH_{s,in}$ = 60% u_s = 2 m/s, and d = 4 mm. Fig. 4 shows the variation of the primary air outlet temperature in 9000 s. The light pink area is the spraying period. Rest of the time is named interval or non-spraying period, corresponding to the light green region. Under the periodic spraying mode, the PIEC is thoroughly wetted to ensure the air can be cooled to the lowest temperature, and then the water supply is interrupted. It can be seen that the temperature drops rapidly from 30℃ to 24.82℃, and it gradually turns up and reaches 25.32℃ due to the insufficient amount of water, which is also the signal (0.5℃ temperature rise threshold) to recover the water spraying. The outlet temperature determines the opening point of the spray system, which eventually forms several cycles within the range of every double-headed arrow. For recurrent spraying conditions, the temperature varies periodically so that any cycle (such as the solid brown line) can be taken for 3E analysis. In this scenario, the water is sprayed for 120 s (pink area) and paused for 2040 s (light green area). While for continuous spraying conditions, the temperature value can be stabilized at the lowest point (such as point A in Fig. 4), and its corresponding inlet and outlet parameters of the heat exchanger are used for 3E evaluation.

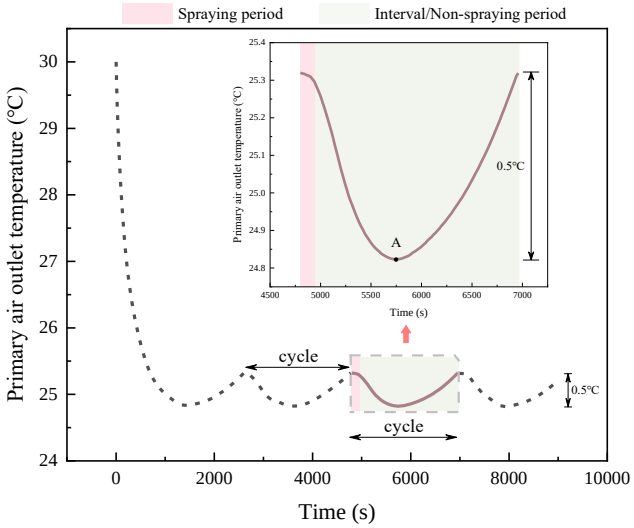

Fig. 4 PIEC primary air outlet temperature profile under periodic spraying

In order to compare the 3E performance under different spraying conditions, the simulations are conducted based on the input parameters listed in Table 2, and the results are used to calculate the 3E indicators in the following section.

Table 2 Range of input parameters for PIEC performance analysis

Parameter	Range	Parameter	Range
$t_{p,in}$ (℃)	24-36	$RH_{s,in}$ (%)	60
$RH_{p,in}$ (%)	40	u_s (m/s)	1-3
u_p (m/s)	1.5-3.5	d (mm)	4, 5
$t_{s,in}$ (℃)	25	L (mm)	400

3. 3E evaluation indicators

3.1 Energy indicator

Three indicators are employed as energy indicators, namely, wet-bulb efficiency, cooling capacity, and *COP*, which have been pervasively used and written from Eq. (16) to Eq. (17) and Eq. (19) [36-38].

$$\eta_{wb} = \frac{t_{p,in} - t_{p,out}}{t_{p,in} - t_{wb,s,in}} \tag{16}$$

$$Q = m_p c_{pa}\left(t_{p,in} - t_{p,out}\right) \tag{17}$$

where $t_{p,out}$ is the outlet temperature in the consecutive spraying circumstances, which needs to be replaced and calculated by Eq. (18) during a ranged cycle in the periodic spraying scenarios.

$$t'_{p,out} = \frac{\int_{\tau_0}^{\tau_2} t_{p,out}\, d\tau}{\tau_2 - \tau_0} \tag{18}$$

where 0 and 2 represent the start and end time of a cycle, respectively.

$$COP = \frac{Q}{W_{fans} + (W_{pump} or\ W_{pump}')} \tag{19}$$

The fan power can be calculated by Eq. () according to the existing IEC literature [3].

$$W_{fan} = \frac{Q\Delta P_i}{\eta_0 \eta_1} \cdot K \tag{20}$$

$$P_i = \frac{f_{Re} L}{ReD_e} \cdot \frac{\rho u^2}{2} \quad (\text{where } i = p, s) \tag{21}$$

$$f_{Re} = 96 * (1 - 1.3553(\frac{L}{d}) + 1.9467\left(\frac{L}{d}\right)^2 - 1.7012\left(\frac{L}{d}\right)^3 + 0.9564\left(\frac{L}{d}\right)^4 - 0.2537\left(\frac{L}{d}\right)^5) \tag{22}$$

where the values of fan power are figured according to the supply air volume and an assumed distribution resistance of 30 Pa for both primary and secondary air loops.

The water pump power in the consistent mode and equivalent power of a cycle under periodic spraying can be obtained by the following equations, which are both related to the head loss of the nozzle, gravity, and valves [39].

$$W_{pump} = m_{sp} \cdot g \cdot h_{total} \cdot K \tag{23}$$

$$W_{pump}' = \frac{\int_{\tau_0}^{\tau_1} m_{sp} \cdot g \cdot h_{total} \cdot K d\tau}{\tau_2 - \tau_0} \tag{24}$$

where 1 represents the timepoint pausing the water spraying; K is the motor capacity coefficient, g is the gravitational acceleration; m_{sp} is the mass flow of the spraying water.

$$h_{total} = h_{nozzle} + h_{gravity} + h_{valve} \tag{25}$$

3.2 Exergy indicator

Exergy can reflect the useful energy of a thermodynamic system compared with the dead/reference state. The total exergy of the moist air is mainly the sum of its thermal exergy, chemical exergy, and mechanical exergy (Eq. (20)), which are accordingly related to the air temperature, moisture content, and pressure (Eq. (21) to Eq. (23)) [35]. Besides, several assumptions can be made prior to calculating the exergy for different operating conditions. Firstly, it has been proved that the energy conversion predominantly leads to the heat and mass transfer in the IEC rather than the work from minor pressure changes. Therefore, the pressure drop is usually ignored in IEC exergy analysis [23]. Secondly, the saturation point of the inlet primary air is determined as the reference/dead state [40]. Thirdly, the tiny convection that arises in the porous layer is not considered. Fourthly, in the continuous mode, the inlet and outlet water status is identical. In the periodic mode, one cycle is taken as the objective for analysis, and the inlet and outlet statuses of the wet porous media are identical. Therefore, the water exergy in the stable spraying mode and the exergy of the wet porous media in the periodic spraying mode are both neglected.

$$Ex = Ex_{ther} + Ex_{chem} + Ex_{mech} \tag{26}$$

$$Ex_{ther} = m(C_{p,a} + \omega C_{p,v})(T - T_0 - T_0 \ln(\frac{T}{T_0})) \tag{27}$$

$$Ex_{chem} = m((1 + 1.608w)T_0 R_a ln\left(\frac{1 + 1.608\omega_0}{1 + 1.608\omega}\right) + 1.608wt_0 R_a ln\left(\frac{\omega}{\omega_0}\right)) \tag{28}$$

$$Ex_{mech} = m(1 + 1.608\omega)R_a T_0 \ln(\frac{p}{p_0})) \tag{29}$$

The exergy balance equation of the PIEC can be formulated by Eq. (24):

$$Ex_{p,in} + Ex_{s,in} - Ex_{p,out} - Ex_{s,out} - Ex_{loss} + Ex_{fan} + Ex_{pump} = 0 \tag{30}$$

When evaluating the exergy performance of the IEC system, the exergy efficiency usually needs to be calculated. Nonetheless, Ratlamwala and Dincer mentioned that the definition of this indicator varies based on different understandings [19]. The commonly-used definitions are: 1) the ratio of output exergy to supply exergy [41, 42]; 2) the ratio of produced exergy by conversion to the supplied exergy for maintaining the transfer process [17, 23]. Recently, the latter one has become popular because the influence of the dead state is handled, which is adopted as Eq. (25) in this study as well. The exergy loss ratio is defined as the exergy loss to the input exergy Eq. (26). [21].

$$\eta_{ex} = \frac{\Delta Ex_p}{\Delta Ex_s + Ex_{fan} + Ex_{pump}} \tag{31}$$

$$\eta_{loss} = \frac{Ex_{loss}}{Ex_{in}} \tag{32}$$

3.3 Environmental indicator

The CO_2 emission, which is the most important when it comes to carbon peaking and carbon neutrality, is determined as the environmental indicator and can be calculated by Eq. (27). In this study, the emission coefficient (f_{CO2}) of CO_2 can be appointed as 0.581 kg/kWh according to the latest notice issued by the official governmental ministry [42].

$$m_{emission} = f_{CO2}E \tag{33}$$

$$E = \frac{Q}{COP}\tau \tag{34}$$

4. Results and discussion

4.1 Energy performance

4.1.1 Influence of the primary air inlet temperature

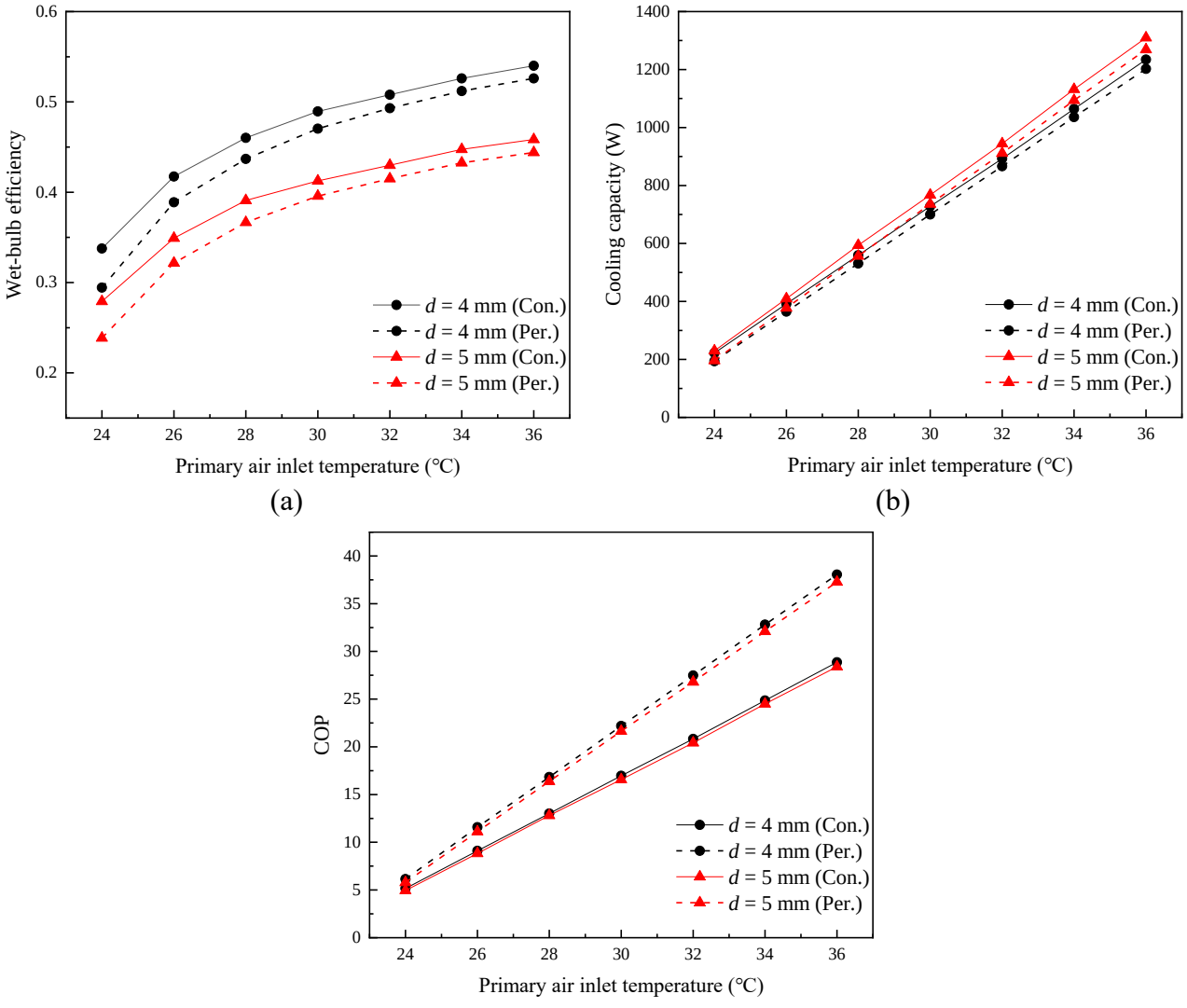

(c)

Fig. 5 Influence of the primary air inlet temperature on (a) Wet-bulb efficiency (b) Cooling capacity, and (c) COP under consistent and periodic spraying

Figs. 5 (a)-(c) show the influence of primary air inlet temperature on the wet-bulb efficiency, cooling capacity, and COP of PIEC under the two spraying modes. It is observed that the trend of the three indicators grows with the higher inlet temperature. The wet-bulb efficiency and cooling capacity under continuous mode are slightly higher than those under intermittent mode. Taking the pair of cases that d = 4 mm as an example, the wet-bulb efficiency (solid black line) increases from 0.34 to 0.54 as input temperature grows from 24℃ to 36℃, which is slightly superior to the values on the black dash line (Fig. 5(a)). The same tendency applies to cooling capacity (Fig. 5(b)), and the values are from 222.26 W to 1234.45 W and 193.72 W to 1202.34 W, respectively. The COP values vary from 5.16 to 28.86 on the dash line, which are greater than those on the solid line. Furthermore, the differences between the two lines are enlarged to 9.2 with the higher inlet temperature, and the growth ratio is up to 36.6% among these cases. To sum up, although the temperature will rise slowly in the non-spraying period, causing the little drop of the first two indicators, the periodic spraying notably improves the COP value and lead to the energy saving benefit.

4.1.2 Influence of the primary air velocity

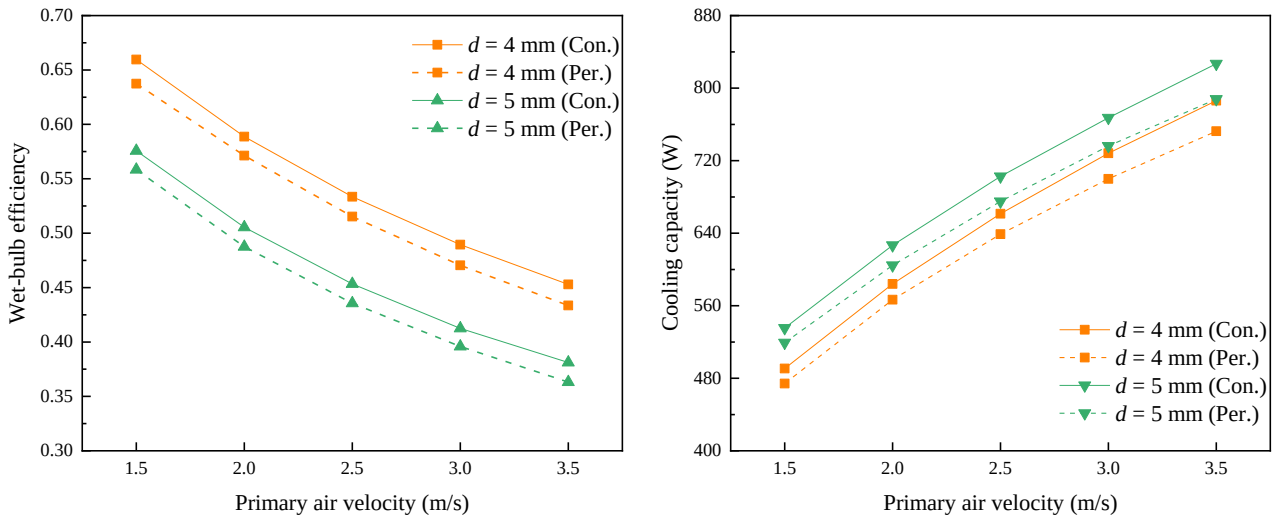

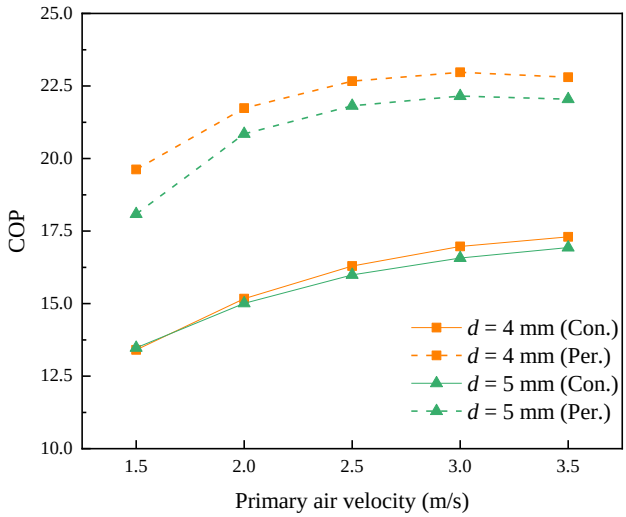

(c)

Fig. 6 Influence of the primary air velocity on (a) Wet-bulb efficiency (b) Cooling capacity, and (c) COP under consistent and periodic spraying

The impact of the primary air velocity on the three indicators is depicted in Fig. 6. It can be found that the wet-bulb efficiency and cooling capacity with consecutive spraying are slightly higher than those in intermittent spraying conditions because the periodic mode cannot always maintain the lowest temperature as it is in the consistent circumstance. However, the tendencies of the three indicators are different. Taking the pair of cases that d = 4 mm for instance, the wet-bulb efficiency (solid orange line) declines significantly from 0.66 to 0.45 with the increase of primary air speed (Fig. 6(a)), and the values on the dash line also fall from 0.64 to 0.43. Nonetheless, the cooling capacity shows an opposite trend and expands from 490.70 W to 798.14 W and from 474.20 W to 752.52 W in the two scenarios, given the faster velocity (Fig. 6(b)). COPs are enhanced by the higher air velocity, but the extent of the growth gradually weakens. The periodic strategy can achieve 32.8% improvement of COP on average compared with the traditional plan (Fig. 6(c)). In short, raising the primary air velocity can stably promote the energy saving of the recurrent spraying plan with a tiny temperature fluctuation, while the further elevation of COP will be quite limited when the speed reaches a certain value.

4.1.3 Influence of the secondary air velocity

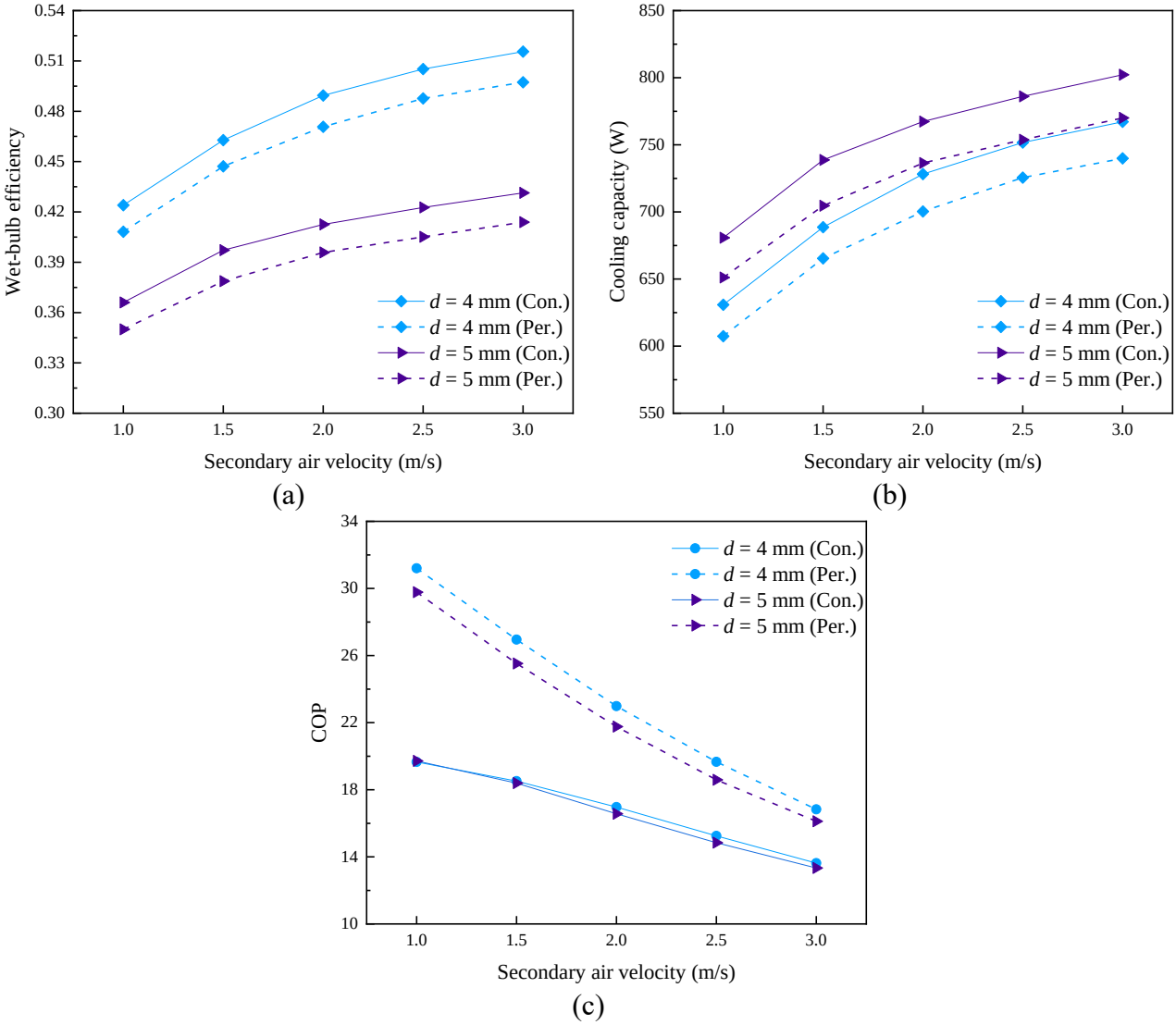

Fig. 7 Influence of the secondary air velocity on (a) Wet-bulb efficiency (b) Cooling capacity, and (c) COP under consistent and periodic spraying

The secondary air velocity is an essential parameter, and the influence of it on the three performance indicators is presented in Fig. 7. By and large, the increasing trend of wet-bulb efficiency and cooling capacity is noticed with the development of the secondary air velocity, and the stable spraying mode contributes to the greater performance. Contrary to the former two indicators, COPs suffer from great loss, and it is visibly upgraded by using the recurrent spraying plan. Taking a couple of scenarios that d = 4 mm as an example, in Figs. 7(a)-(b), the points on the solid blue line are larger than those on the dash blue line, and the best wet-bulb efficiency and cooling capacity are 0.43 and 767.12 W under the stable spraying mode. The maximum COP is obtained as 31.2 when the velocity is 1 m/s, which is 58.7% more than the traditional condition. Nonetheless, the COP improvement shrinks rapidly with the air speed from 1 m/s to 3 m/s in the two pairs of scenarios. The ability to reduce the outlet temperature is limited by increasing the secondary air speed. Meanwhile, the energy

consumption of the secondary air due to the need to overcome the resistance from the spray water is more than the energy saved by the periodic spray. These two reasons together cause the COP to decline along with the increase of the secondary air velocity. Thus, it needs prudent consideration to raise the velocity to reduce the outlet temperature, which may lead to a lower system COP.

4.2 Exergy performance

4.2.1 Exergy flow and distribution

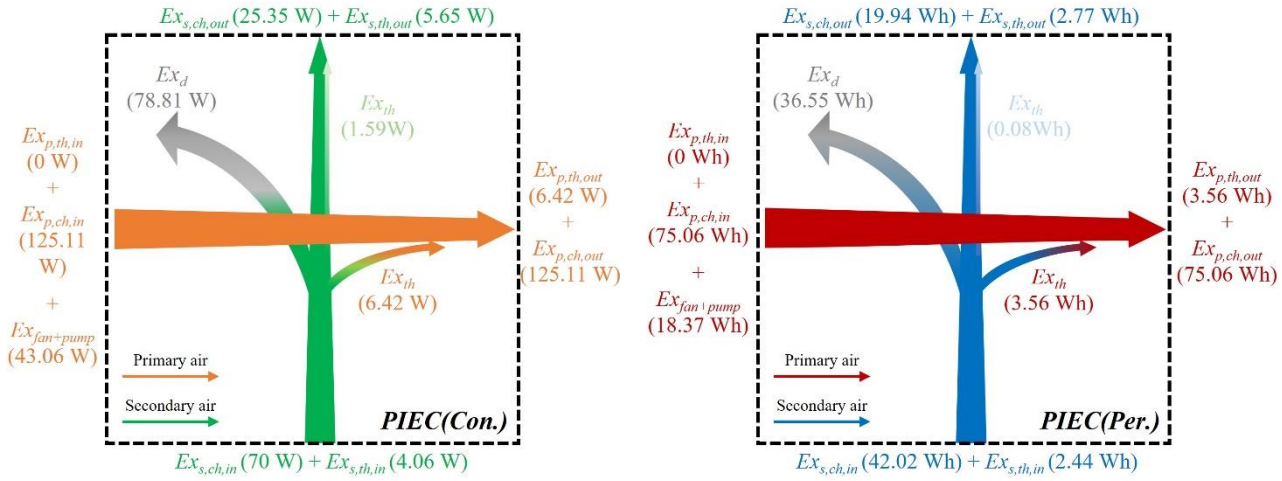

(a) (b)

Fig. 8 Exergy flow variation of PIEC in the condition of (a) consistent spraying and (b) periodic spraying

The exergy flow variations of two example cases of the PIEC are presented in Fig. 8 under two spraying conditions. The input parameters are fixed as: $t_{p,in}$ = 30°C, $RH_{p,in}$ = 40%, u_p =3 m/s, $t_{s,in}$ = 25°C, $RH_{s,in}$ = 60% u_s = 2 m/s, d = 4 mm. For continuous spraying mode, the whole process relies on the transformation of the secondary air chemical exergy, which has three destinations: primary air thermal exergy, secondary air thermal exergy, and destruction. The former two items are the majority of the conversion. In Fig. 8(a), there is 6.42 W thermal exergy converted to the primary air. Meanwhile, the secondary air gains 1.59W thermal exergy and reaches 5.65 W, accompanied by the rapid reduction of secondary air chemical exergy from 70 W to 25.35 W. The primary air chemical exergy remains the same because there is no moisture content change. For each cycle generated under intermittent spraying conditions, the variation trend is similar to that of traditional spraying. As shown in Fig. 8(b), the primary air acquires 3.56 Wh of thermal exergy, while the chemical exergy remains fixed. The thermal exergy of the secondary air increases slightly from 2.44 Wh to 2.77 Wh, while the chemical exergy decreases significantly from 42.02 Wh to 19.94 Wh. The mechanical exergy is to maintain the fluid flowing, which can be regarded that has no influence on the value of the air thermal and chemical exergy. In addition, it is noticed that destruction inevitably exists no matter which spraying conditions, indicating the irreversibility of the whole process. The exergy efficiency and loss ratio are discussed in the following sections with varied input air conditions.

4.2.2 Influence of the primary air inlet temperature

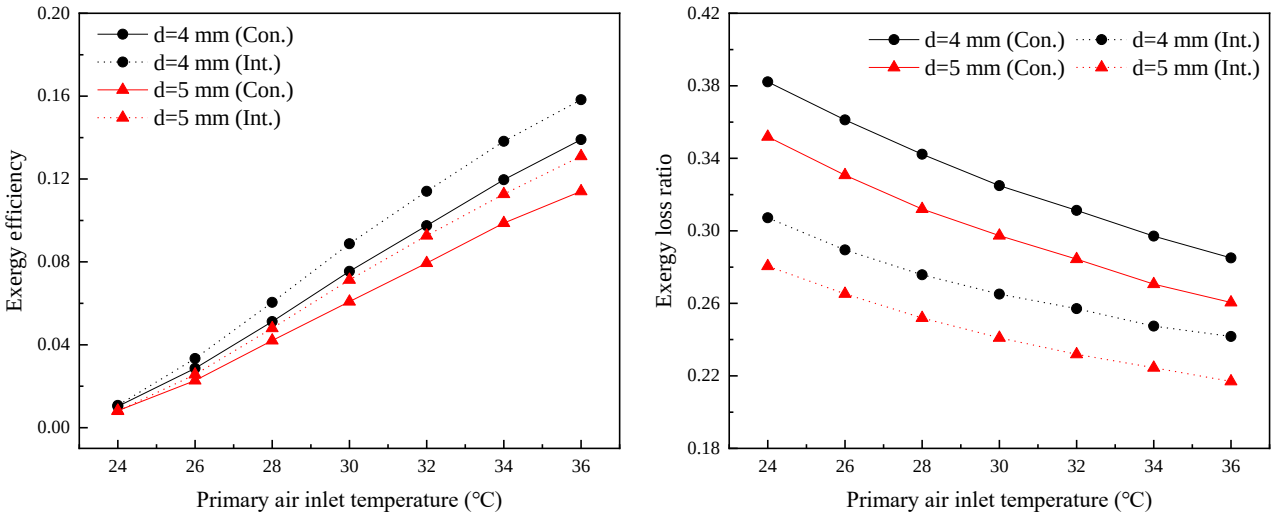

Fig. 9 Influence of the primary air inlet temperature on (a) exergy efficiency (b) exergy loss ratio under consistent and periodic spraying

As mentioned in section 3.2, the saturation point of the inlet primary air is determined as the reference state for exergy performance calculation. The temperature and humidity ratio of the dead state increases with the growing inlet temperature. Therefore, the primary air absorption ability, the secondary air absorption ability, and the cooling ability of secondary air are relatively enhanced. The exergy efficiency and exergy loss ratio are used as indicators to examine the exergy performance of the PIEC in two spraying modes. The impact of the primary air inlet temperature on two indicators is shown in Fig. 9. The higher inlet temperature leads to the greater exergy efficiency, while it the exergy loss ratio varies concurrently. For the exergy efficiency, the red and black dash curves are above the solid lines, indicating the enhancement by the periodic spraying. Regarding the exergy loss ratio, the scenarios of intermittent strategies achieve lower values on average and perform better than the conventional mode. The reduction of the loss ratio is 0.07 and 0.06 on average in the scenarios of d = 4 mm and d = 5 mm, respectively.

The inlet exergy of primary air and secondary air under the two spraying modes is identical, so the exergy efficiency depends on the variation extent of the other two outlet exergy. Although the primary air under traditional mode can obtain a little more exergy, the exergy consumed from the secondary side under continuous spraying is more than that under periodic spraying mode. In other words, under periodic spraying mode, the acquired primary air exergy is slightly low, but the consumed exergy from the secondary air is much lower than the traditional mode, resulting in the better exergy efficiency. For the PIEC, the humidity difference between the water membrane and secondary air decreases with the limited water evaporation during the non-spraying duration. Meanwhile, the lack of water leads to the temperature increase of the heat transfer plate, and the temperature difference between the primary air and plate is smaller. These two fewer differences diminish the exergy loss

ratio in the periodic spraying cases.

4.2.2 Influence of the primary air velocity

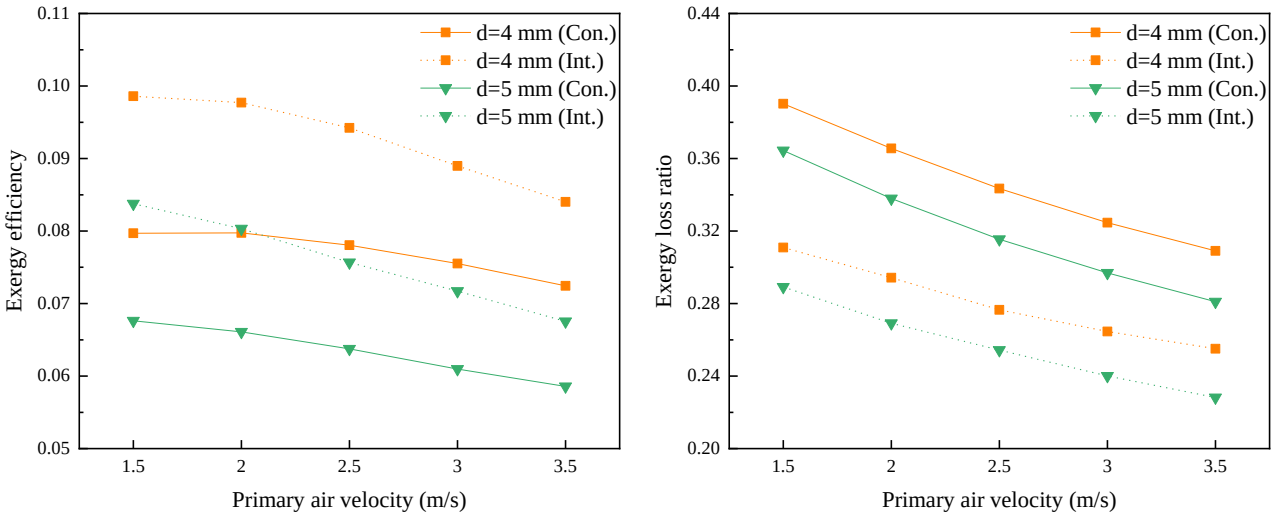

Fig. 10 Influence of the primary air velocity on (a) exergy efficiency (b) exergy loss ratio under consistent spraying and periodic spraying

The impact of the primary air velocity on exergy efficiency and exergy loss ratio under two spraying modes is shown in Fig. 10. The two indicators drop with the primary air velocity development. Periodic spraying cases show the higher exergy efficiency and exergy loss ratio compared with the traditional mode. Taking the pair of cases of d = 4 mm as an example, the exergy efficiency falls from 0.08 to 0.07 with the growing speed from 1.5 m/s to 3.5 m/s, exceeding the solid line (Fig. 10(a)). Regarding the exergy loss ratio, it can be seen from Fig. 10(b) that dash lines are below the solid line, which means that the period spraying can reduce the exergy loss ratio. The loss ratio under consistent mode decreases from 0.39 to 0.31, while the range is 0.31 to 0.26 in the periodic conditions.

Given the same inlet temperature, the higher primary air speed leads to the larger total inlet exergy as well as the exergy destruction. The degree of the obtained exergy in the primary air is still less than that of the converted exergy from the secondary air so that the declining tendency occurs in Fig. 10(a). The increasing degree of the total inlet exergy is much greater than the exergy loss, which leads to the decreasing trend along the X-axis from the left side in Fig. 10(b). When the periodic spraying is implemented, the humidity gradient between the secondary air and the water film is narrowed due to the limited water reserved by PIEC in the whole cycle. Although the exergy obtained by the primary air decreases slightly, the exergy efficiency is still improved compared with continuous spraying. The periodic spraying reduces the temperature difference between the plate and the primary air as well as the moisture content difference of the secondary air, which promotes the decrease of the exergy loss ratio.

4.2.3 Influence of the secondary air velocity

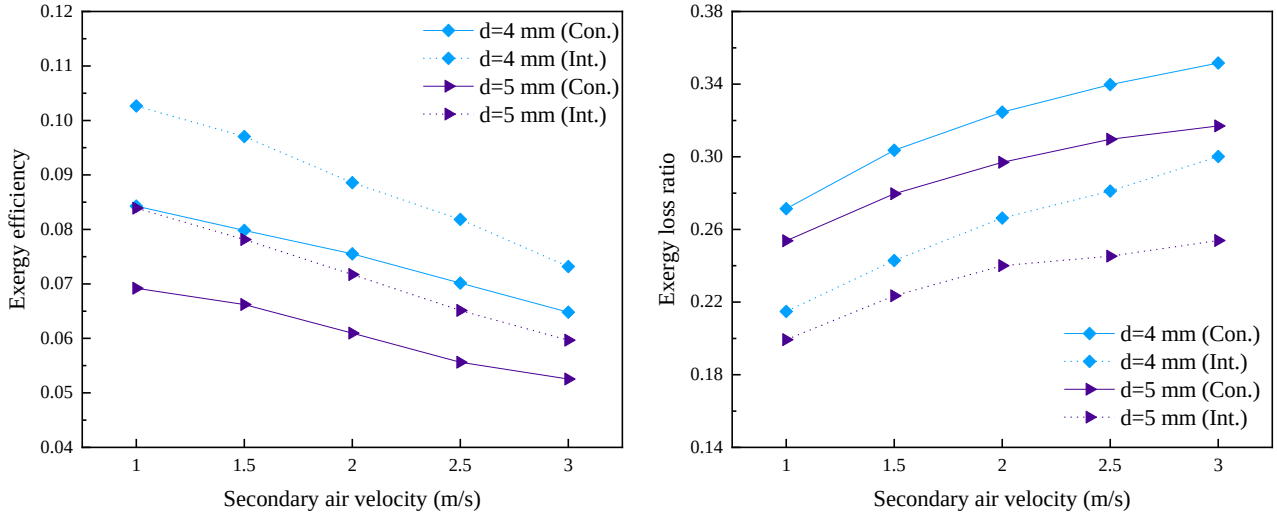

(a) (b)

Fig. 11 Influence of the secondary air velocity on (a) exergy efficiency (b) exergy loss ratio under consistent spraying and periodic spraying

Figs. 11(a)-(b) exhibit the impact of the secondary air velocity on exergy efficiency and exergy loss ratio under conventional spraying and recurrent spraying. It is found that the two indicators have the opposite trend with the growing secondary air speed from 1 m/s to 3 m/s. Taking the couple cases of d = 4 mm for discussion, the exergy efficiency declines from 0.084 to 0.064 and from 0.102 to 0.073 for persistent and periodic modes. The exergy loss ratio increases up to 0.197 and 0.157 with the faster speed of 3 m/s, respectively. It is found that the dash exergy efficiency curves are higher but the corresponding exergy loss ratio is lower, indicating the better performance using the periodic spraying plan.

The faster secondary air augments the entire input exergy. However, it has been mentioned in section 4.1.3 that reducing the primary air outlet temperature is limited by increasing of secondary air speed. Therefore, the degree of exergy obtained by primary air is smaller than the exergy consumption of secondary air growth, leading to the situation that the exergy efficiency decreases all the way. In addition, the increase of the secondary air velocity can enlarge the moisture content difference between the secondary air and the water membrane, which enhances water evaporation and takes away more latent heat. The plate temperature decreases, and the gradient between it and primary air is expanded. The above two potential differences lead to bigger exergy loss ratio. When intermittent spraying is used, the results resemble the previous two influencing factors. The moisture content potential between the water film and secondary air shrinks because of the gradual evaporation of the remaining water, and the rising plate temperature brings the closer temperature difference between the plate and the primary air. Compared with traditional spraying, the two potential differences both dwindle, thus reducing the exergy loss ratio.

4.2.4 Sensitivity analysis on the exergy indicators

Sensitivity analysis is essential to tell the influence degree of the input parameters on the performance indicators [43]. Therefore, the analysis is conducted for the exergy efficiency and exergy loss ratio based on the three ranged parameters (primary air inlet temperature, primary air velocity, and secondary air velocity) in section 4.2. The basic procedures are illustrated as follows. Firstly, two curves are fitted according to the obtained output results of the two indicators and input parameters. Secondly, the corresponding parameters are taken as partial derivatives using the fitting formula, and six new equations are accordingly obtained. Thirdly, more discrete points of primary air inlet temperature, the primary air velocity, and secondary air velocity within the range in Table 2 are input into the equations. Finally, the three curves are obtained and normalized, which are presented in one figure for each exergy indicator [44, 45].

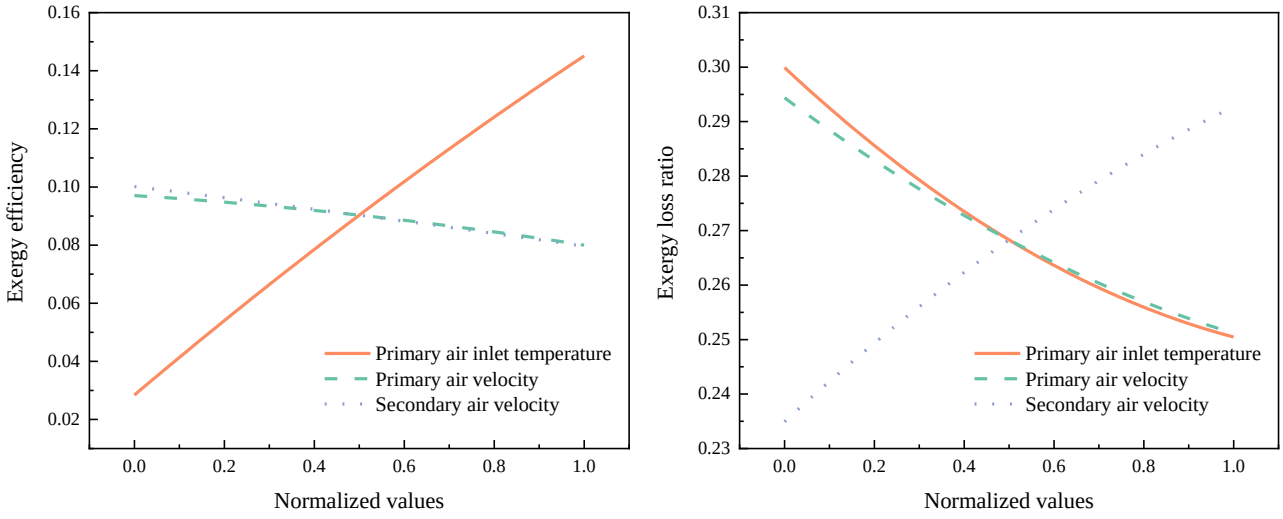

(a) (b)

Fig. 12 Sensitivity analysis of the ranged parameters for (a) exergy efficiency (b) exergy loss ratio

The steepness of curves can be used to judge and rank the sensitivity of input parameters, and the positive and negative slope values reveal the variation trends [46]. It can be observed from Fig. 12(a) that the solid orange curve is much steeper than primary air and secondary air velocities, indicating the higher sensitivity of primary air inlet temperature for exergy efficiency. Besides, the positive slope means that the temperature growth increases exergy efficiency, while the other two have the opposite tendencies. Regarding the exergy loss ratio (Fig. 12(b)), the steepness of secondary air velocity is slightly higher than primary air inlet temperature and primary air velocity, which means that it has the most significant sensitivity. In addition, enhancing the secondary air velocity leads to a higher exergy loss ratio as the slope is positive, while the other two factors hold reverse tendencies.

4.3 Environmental evaluation

As discussed in section 4.1, owing to the advantageous COP values, the PIEC can treat the cooling load at the cost of lower energy under both consistent and periodic spraying modes so as to indirectly mitigate greenhouse gas emissions. It is assumed that the PIEC handles the same cooling load (1 kW) under the dual spraying modes for environmental evaluation. The annual operation time of the AC

system is set as 1200 h. The estimated CO_2 emissions of the PIEC in the ranged primary air inlet temperature are displayed in Fig. 13.

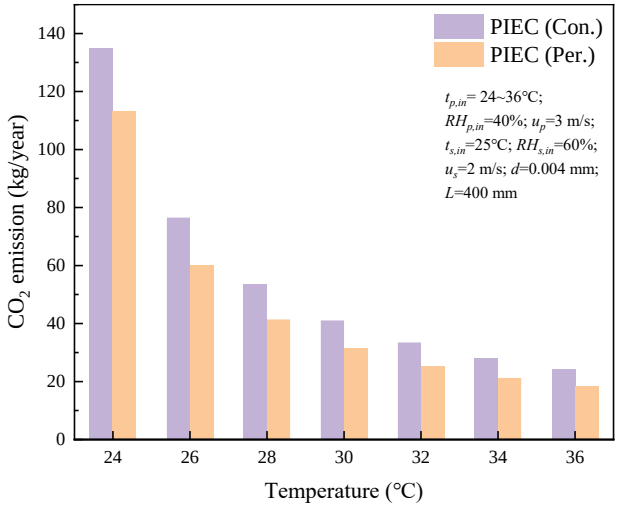

Fig. 13 CO_2 emission of the traditional AC and the PIEC under dual spraying modes

As shown in Fig. 13, the operating energy is further lessened by the periodic spraying strategy, which reduces with the growing temperature. The annual CO_2 emission of PIEC under periodic spraying can be decreased by the range from 16% to 24.2% compared with the consistent spraying for every kilowatt cooling load, indicating favorable environmental benefits.

5. Limitations and future works

By reason of the improved water retention capacity of the porous layer, the performance of the PIEC can be maintained under the spraying mode, and the outlet temperature growth can be postponed. However, the limitation of this study needs to be noted. Although the hybrid porous plate can be fabricated by sintering the porous layer on the bare plate, the overall price is more expensive than the normal IEC. Therefore, the economic analysis is not presented due to the customization and non-commercialization of the PIEC. The next step will focus on finding lower-priced plates and simplifying the manufacturing procedures, which may significantly cut down the initial cost of the PIEC for better product promotion to the market. In addition, the IEC usually handles the air under hot and arid climate conditions with no moisture content change in the fresh air channel, and the influence of humidity is not considered in this study. When it is under hot-humid areas, this requires further discussion. The “E” performance of other configurations, such as counter/parallel PIECs or PIECs with other shapes, are not included and compared in this study, which is going to be carried out in our future work.

6. Conclusions

This study presented the energy, exergy, and environmental (3E) analysis of a proposed indirect evaporative cooler incorporated with porous layer (PIEC). The porous layer on the secondary air channel collects the spraying water, while the bare surface is towards the primary air side. The PIEC

model was briefly introduced, and comparisons of its performance were conducted from 3E perspectives under consistent spraying and unique periodic spraying modes. The main conclusions are summarized as follows.

1) The consistent spraying maintains the performance constant because of the sufficient water supply. During the non-spraying period, the stored water in the wet porous media can temporarily maintain the evaporation process for air cooling and delay the temperature rise. Under the intermittent spraying condition, the outlet temperature can be controlled to fluctuate within the threshold and generate small cycles.

2) The larger wet-bulb efficiency can be obtained with the higher primary air inlet temperature, lower primary air velocity, and faster secondary air velocity under the continuous spraying. The cooling capacity can be enhanced by the greater primary air inlet temperature and faster air speed in two channels. However, the periodic spraying plan can substantially improve the COPs by up to 58.1% among the studied cases at the cost of tiny temperature fluctuation, which can be employed in situations regarding energy saving as the priority.

3) In both two spraying modes, the greater primary air inlet temperature and lower air velocities in two channels can contribute to a higher exergy efficiency, while the lower exergy loss ratio happens in the cases with low primary air inlet temperature, fast primary air velocity, and slow secondary air velocity. Furthermore, using the periodic spraying mode can not only enhance the exergy efficiency and lessen the exergy loss ratio, but also achieve higher energy saving performance than the consistent spraying mode, which is owing to the reduction of temperature potential difference in the primary air side and humidity potential difference in the secondary air side.

4) The periodic spraying strategy further shortens the operating energy. The annual CO_2 emission of the PIEC under periodic spraying can be reduced by the range from 16% to 24.2% compared with the traditional consistent spraying for every kilowatt cooling load, indicating the greater environmental benefit.

CRediT authorship contribution statement

Wenchao Shi: Conceptualization; Methodology; Program; Formal analysis; Writing – original draft. **Hongxing Yang:** Conceptualization; Supervision; Funding acquisition; Writing – review & editing; **Xiaochen Ma:** Validation; Data curation; Resources; **Xiaohua Liu:** Methodology; Writing – review & editing; Supervision.

Declaration of competing interest

The authors declare that they have no known competing financial interests or personal relationships that could have appeared to influence the work reported in this paper.

Acknowledgment

The authors wish to acknowledge the financial support provided by the General Research Fund projects of the Hong Kong Research Grant Council (Ref. No.: 15213219 and 15200420).

References

[1] Q. Chen, Z. Kuang, X. Liu, and T. Zhang, "Energy storage to solve the diurnal, weekly, and seasonal mismatch and achieve zero-carbon electricity consumption in buildings," *Applied Energy,* vol. 312, p. 118744, 2022/04/15/ 2022.

[2] Q. Chen, Z. Kuang, X. Liu, and T. Zhang, "Transforming a solar-rich county to an electricity producer: Solutions to the mismatch between demand and generation," *Journal of Cleaner Production,* vol. 336, p. 130418, 2022/02/15/ 2022.

[3] X. Ma, W. Shi, and H. Yang, "Study on water spraying distribution to improve the energy recovery performance of indirect evaporative coolers with nozzle arrangement optimization," *Applied Energy,* vol. 318, 2022.

[4] Y. Min, Y. Chen, W. Shi, and H. Yang, "Applicability of indirect evaporative cooler for energy recovery in hot and humid areas: Comparison with heat recovery wheel," *Applied Energy,* vol. 287, 2021.

[5] E. Katramiz, H. Al Jebaei, S. Alotaibi, W. Chakroun, N. Ghaddar, and K. Ghali, "Sustainable cooling system for Kuwait hot climate combining diurnal radiative cooling and indirect evaporative cooling system," *Energy,* vol. 213, p. 119045, 2020/12/15/ 2020.

[6] Y. Al Horr, B. Tashtoush, N. Chilengwe, and M. Musthafa, "Operational mode optimization of indirect evaporative cooling in hot climates," *Case Studies in Thermal Engineering,* vol. 18, p. 100574, 2020/04/01/ 2020.

[7] Y. Zhang, H. Zhang, H. Yang, Y. Chen, and C. W. Leung, "Counter-crossflow indirect evaporative cooling-assisted liquid desiccant dehumidifier: Model development and parameter analysis," *Applied Thermal Engineering,* vol. 217, p. 119231, 2022/11/25/ 2022.

[8] A. Adam, D. Han, W. He, M. Amidpour, and H. Zhong, "Numerical investigation of the heat and mass transfer process within a cross-flow indirect evaporative cooling system for hot and humid climates," *Journal of Building Engineering,* vol. 45, p. 103499, 2022/01/01/ 2022.

[9] H. Zhang, H. Ma, S. Ma, and M. Yang, "Investigation on the performance of an indirect evaporative cooling system integrated with liquid dehumidification," *Energy and Buildings,* vol. 251, p. 111356, 2021/11/15/ 2021.

[10] D. Pandelidis *et al.*, "Performance analysis of rotary indirect evaporative air coolers," *Energy Conversion and Management,* vol. 244, p. 114514, 2021/09/15/ 2021.

[11] C. Deepak, R. Naik, S. C. Godi, C. K. Mangrulkar, and P. H.K, "Thermal performance analysis of a mixed-flow indirect evaporative cooler," *Applied Thermal Engineering,* vol. 217, p. 119155, 2022/11/25/ 2022.

[12] J. Lin, K. Thu, S. Karthik, M. W. Shahzad, R. Wang, and K. J. Chua, "Understanding the transient behavior of the dew point evaporative cooler from the first and second law of thermodynamics," *Energy Conversion and Management,* vol. 244, p. 114471, 2021/09/15/ 2021.

[13] W. Shi, X. Ma, Y. Gu, Y. Min, and H. Yang, "Indirect evaporative cooling maps of China: Optimal and quick performance identification based on a data-driven model," *Energy Conversion and Management,* vol. 268, 2022.

[14] S. Rasheed, M. Ali, H. Ali, and N. A. Sheikh, "Experimental evaluation of indirect evaporative cooler with improved heat and mass transfer," *Applied Thermal Engineering,* vol. 217, p. 119152, 2022/11/25/ 2022.

[15] S. Kashyap, J. Sarkar, and A. Kumar, "Experimental exergy, economic and sustainability analyses of the dual-mode evaporative cooler," *International Journal of Refrigeration,* vol. 135, pp. 121-130, 2022.

[16] Y. Cui, J. Zhu, S. Zoras, and L. Liu, "Review of the recent advances in dew point evaporative cooling

technology: 3E (energy, economic and environmental) assessments," *Renewable and Sustainable Energy Reviews,* vol. 148, p. 111345, 2021/09/01/ 2021.

[17] J. Lin, D. T. Bui, R. Wang, and K. J. Chua, "On the exergy analysis of the counter-flow dew point evaporative cooler," *Energy,* vol. 165, pp. 958-971, 2018/12/15/ 2018.

[18] W. Li, Y. Li, W. Shi, and J. Lu, "Energy and exergy study on indirect evaporative cooler used in exhaust air heat recovery," *Energy,* vol. 235, p. 121319, 2021/11/15/ 2021.

[19] T. A. H. Ratlamwala and I. Dincer, "Efficiency assessment of key psychometric processes," *International Journal of Refrigeration,* vol. 36, no. 3, pp. 1142-1153, 2013.

[20] R. Kousar, M. Ali, M. K. Amjad, and W. Ahmad, "Energy, Exergy, Economic, Environmental (4Es) comparative performance evaluation of dewpoint evaporative cooler configurations," *Journal of Building Engineering,* vol. 45, p. 103466, 2022/01/01/ 2022.

[21] H. Zhang, H. Ma, and S. Ma, "Energy, exergy, economic and environmental analysis of an indirect evaporative cooling integrated with liquid dehumidification," *Energy,* vol. 253, p. 124147, 2022/08/15/ 2022.

[22] V. V. Rao and S. P. Datta, "Experimental evaluation of energetic and exergetic enactment for exotic evaporative to expansion-type edifice-coolers," *International Communications in Heat and Mass Transfer,* vol. 135, p. 106064, 2022/06/01/ 2022.

[23] Y. Yang, C. Ren, C. Yang, M. Tu, B. Luo, and J. Fu, "Energy and exergy performance comparison of conventional, dew point and new external-cooling indirect evaporative coolers," *Energy Conversion and Management,* vol. 230, p. 113824, 2021/02/15/ 2021.

[24] S. Kashyap, J. Sarkar, and A. Kumar, "Effect of surface modifications and using hybrid nanofluids on energy-exergy performance of regenerative evaporative cooler," *Building and Environment,* vol. 189, p. 107507, 2021/02/01/ 2021.

[25] S. Kashyap, J. Sarkar, and A. Kumar, "Exergy, economic, environmental and sustainability analyses of possible regenerative evaporative cooling device topologies," *Building and Environment,* vol. 180, 2020.

[26] H. Yang, W. Shi, Y. Chen, and Y. Min, "Research development of indirect evaporative cooling technology: An updated review," *Renewable and Sustainable Energy Reviews,* vol. 145, 2021.

[27] J. Lv, H. Xu, M. Zhu, Y. Dai, H. Liu, and Z. Li, "The performance and model of porous materials in the indirect evaporative cooling system: A review," *Journal of Building Engineering,* vol. 41, p. 102741, 2021/09/01/ 2021.

[28] Y. Chen, X. Huang, T. Sun, and J. Chu, "Experimental study of plant fiber-polymer composite for indirect evaporative cooler application," *Applied Thermal Engineering,* vol. 199, p. 117543, 2021/11/25/ 2021.

[29] W. Shi, Y. Min, X. Ma, Y. Chen, and H. Yang, "Performance evaluation of a novel plate-type porous indirect evaporative cooling system: An experimental study," *Journal of Building Engineering,* vol. 48, 2022.

[30] W. Shi, Y. Min, Y. Chen, and H. Yang, "Development of a three-dimensional numerical model of indirect evaporative cooler incorporating with air dehumidification," *International Journal of Heat and Mass Transfer,* vol. 185, 2022.

[31] W. Shi, Y. Min, X. Ma, Y. Chen, and H. Yang, "Dynamic performance evaluation of porous indirect evaporative cooling system with intermittent spraying strategies," *Applied Energy,* vol. 311, 2022.

[32] T. Sun, X. Huang, Y. Qu, F. Wang, and Y. Chen, "Theoretical and experimental study on heat and mass transfer

of a porous ceramic tube type indirect evaporative cooler," *Applied Thermal Engineering,* vol. 173, p. 115211, 2020/06/05/ 2020.

[33] R. Boukhanouf, A. Alharbi, O. Amer, and H. G. Ibrahim, "Experimental and Numerical Study of a Heat Pipe Based Indirect Porous Ceramic Evaporative Cooler," *International Journal of Environmental Science and Development,* vol. 6, no. 2, pp. 104-110, 2015.

[34] A. Pakari and S. Ghani, "Comparison of 1D and 3D heat and mass transfer models of a counter flow dew point evaporative cooling system: Numerical and experimental study," *International Journal of Refrigeration,* vol. 99, pp. 114-125, 2019/03/01/ 2019.

[35] S. Kashyap, J. Sarkar, and A. Kumar, "Exergy, economic, environmental and sustainability analyses of possible regenerative evaporative cooling device topologies," *Building and Environment,* vol. 180, p. 107033, 2020/08/01/ 2020.

[36] J. Chu, W. Xu, Y. Fu, and H. Huo, "Experimental research on the cooling performance of a new regenerative dew point indirect evaporative cooler," *Journal of Building Engineering,* vol. 43, p. 102921, 2021/11/01/ 2021.

[37] Y. Wan, Z. Huang, A. Soh, and K. Jon Chua, "On the performance study of a hybrid indirect evaporative cooling and latent-heat thermal energy storage system under commercial operating conditions," *Applied Thermal Engineering,* vol. 221, p. 119902, 2023/02/25/ 2023.

[38] Q. Chen *et al.*, "Experimental study of a sustainable cooling process hybridizing indirect evaporative cooling and mechanical vapor compression," *Energy Reports,* vol. 8, pp. 7945-7956, 2022/11/01/ 2022.

[39] Y. Chen, Y. Luo, and H. Yang, "A simplified analytical model for indirect evaporative cooling considering condensation from fresh air: Development and application," *Energy and Buildings,* vol. 108, pp. 387-400, 2015.

[40] C. Ren, N. Li, and G. Tang, "Principles of exergy analysis in HVAC and evaluation of evaporative cooling schemes," *Building and Environment,* vol. 37, no. 11, pp. 1045-1055, 2002/11/01/ 2002.

[41] H. Caliskan, I. Dincer, and A. Hepbasli, "A comparative study on energetic, exergetic and environmental performance assessments of novel M-Cycle based air coolers for buildings," *Energy Conversion and Management,* vol. 56, pp. 69-79, 2012.

[42] H. Caliskan, I. Dincer, and A. Hepbasli, "Exergoeconomic, enviroeconomic and sustainability analyses of a novel air cooler," *Energy and Buildings,* vol. 55, pp. 747-756, 2012.

[43] Y. Chen, H. Yang, and Y. Luo, "Parameter sensitivity analysis and configuration optimization of indirect evaporative cooler (IEC) considering condensation," *Applied Energy,* vol. 194, pp. 440-453, 2017/05/15/ 2017.

[44] Q. Chen, J. Bi, Y. Zhou, X. Liu, X. Wu, and R. Chen, "Multi-objective Optimization of Spray Drying of Jujube (Zizyphus jujuba Miller) Powder Using Response Surface Methodology," *Food and bioprocess technology,* vol. 7, no. 6, pp. 1807-1818, 2014.

[45] Stat-Ease, "Design - Expert Version 12," 2019.

[46] W. Yan, X. Meng, X. Cui, Y. Liu, Q. Chen, and L. Jin, "Evaporative cooling performance prediction and multi-objective optimization for hollow fiber membrane module using response surface methodology," *Applied Energy,* vol. 325, p. 119855, 2022/11/01/ 2022.